Fluorescent Agonists for the Torpedo Nicotinic Acetylcholine Receptor

Florian Krieger,*[a] Alexandre Mourot,[b] Romulo Araoz,[c] Florence Kotzyba-Hibert,[a] Jordi Molgó,[c] Ernst Bamberg,[b] and Maurice Goeldner[a]

We have synthesized a series of fluorescent acylcholine derivatives carrying different linkers that vary in length and structure and connect the acylcholine unit to the environment-sensitive fluorophores 7-(diethylamino)coumarin-3-carbonyl (DEAC) or N-(7-nitrobenz-2-oxa-1,3-diazol-yl) (NBD). The pharmacological properties of the fluorescent analogues were investigated on heterologously expressed nicotinic acetylcholine receptor (nAChR) from Torpedo californica and on oocytes transplanted with nAChR-rich Torpedo marmorata membranes. Agonist action strongly depends on the length and the structure of the linker. One particular analogue, DEAC-Gly-C6-choline, showed partial agonist be-

havior with about half of the maximum response of acetylcholine, which is at least 20 times higher than those observed with previously described fluorescent dansyl- and NBD-acylcholine analogues. Binding of DEAC-Gly-C6-choline to Torpedo nAChR induces a strong enhancement of fluorescence intensity. Association and displacement kinetic experiments revealed dissociation constants of 0.5 nM for the $\alpha\delta$-binding site and 15.0 nM for the $\alpha\gamma$-binding site. Both the pharmacological and the spectroscopic properties of this agonist show great promise for characterizing the allosteric mechanism behind the function of the Torpedo nAChR, as well as for drug-screening studies.

Introduction

Nicotinic acetylcholine receptors (nAChRs) are ligand-gated ion channels that mediate signal transduction in the post-synaptic membrane. Neurotransmitter binding to the nAChR is a key event for triggering the ionic flux through a cascade of conformational transitions, acting nearly perfectly within the limits prescribed by physical constraints.[1] Most of what we know about nAChRs has been obtained from studies on receptors from Torpedo electric organs or vertebrate neuromuscular junctions.[2–5] This muscle type receptor is a heteropentamer with $\alpha_2\beta\gamma\delta$ stoichiometry and carries two acetylcholine (ACh) binding sites located at the $\alpha\gamma$- and $\alpha\delta$-subunit interfaces. Electrophysiology studies have revealed that binding of the neurotransmitter ACh leads to a rapid opening of the channel, followed by processes of desensitization.[6–8] Recently, a refined structural model of the Torpedo nAChR at 4 Å resolution allowed the description of the receptor in a closed-channel conformation and provided new hypotheses concerning the coupling between agonist binding and channel opening.[9, 10] Although allosteric models of nAChR functioning are well established,[3] knowledge of how agonist binding elicits channel gating remains vague, because the time-resolved detection and analysis of binding in combination with electrophysiology experiments are still limited.[11, 12]

Fluorescence-based detection techniques have opened new avenues for the direct observation of ligand binding, as well as of conformational reorganization of receptors, to be made in a new way.[13] In a recent study, fluorescence measurements were used in combination with electrophysiology to determine the microscopic equilibrium constants for ligand binding to channel gating at the cyclic-nucleotide-gated channel CNGA2.[14] Such studies require the development of fluorescent

agonists that display high efficacy, and these are still not available for the Torpedo nAChR. For more than thirty years, many attempts have been made to functionalize ACh with fluorophores.[15–18] Dansyl- and NBD-acylcholine derivatives have been synthesized for biophysical investigations using fluorescence intensity, fluorescence resonance energy transfer, and time-resolved fluorescence spectroscopy on receptor-enriched membranes from Torpedo electric organs.[19–26] Despite extensive studies in the areas of ligand binding and characterization of the receptor conformational transitions, no data on the pharmacological properties of these fluorescent probes are available. So far, the photolabel AC5 is the only ACh-based photoprobe displaying full agonist properties on Torpedo receptor.[27] A series of fluorescent agonists based on the alkaloid epibatidine and displaying exceptional pharmacological properties for neuronal and neuromuscular nAChRs have recently been described.[28] These new findings encouraged us to syn-

[a] Dr. F. Krieger, Dr. F. Kotzyba-Hibert, Prof. M. Goeldner
Laboratoire de Chimie Bioorganique UMR 7175 LC1 CNRS
Faculté de Pharmacie, Université Louis Pasteur Strasbourg
74, Route du Rhin, BP24, 67401 Illkirch Cedex (France)
Fax: (+33) 390-244-306
E-mail: krieger@bioorga.u-strasbg.fr

[b] Dr. A. Mourot, Prof. Dr. E. Bamberg
Department of Biophysical Chemistry, Max-Plank-Institute of Biophysics
Max-von-Laue-Strasse 3, 60438 Frankfurt am Main (Germany)

[c] Dr. R. Araoz, Dr. J. Molgó
Laboratoire de Neurobiologie Cellulaire et Moléculaire, UPR 9040
Institut Fédératif de Neurobiologie Alfred Fessard
1, Avenue de la Terrasse, 91198 Gif sur Yvette Cedex (France)

Supporting information for this article is available on the WWW under http://www.chembiochem.org or from the author.

thesize and to characterize new fluorescent agonists structurally related to the neurotransmitter ACh. Such probes are extremely useful for describing the microscopic equilibrium and rate constants for agonist binding and channel gating of the *Torpedo* nAChR, as well as for subsequent development of drug-screening assays.

Here we report on the synthesis and the pharmacological and spectroscopic characterization of fluorescent acylcholines. In addition, we have reinvestigated the pharmacological properties of two classes of previously described fluorescent acylcholines.[18,29] We show that one of our new compounds—DEAC-G-C6-Ch (**14**; Scheme 1 C)—binds and activates the *Torpedo* nAChR remarkably more efficaciously than the fluorescent acylcholines described previously. Association and displacement kinetics revealed subnanomolar affinities and a strong site-selectivity for desensitized *Torpedo* nAChR.
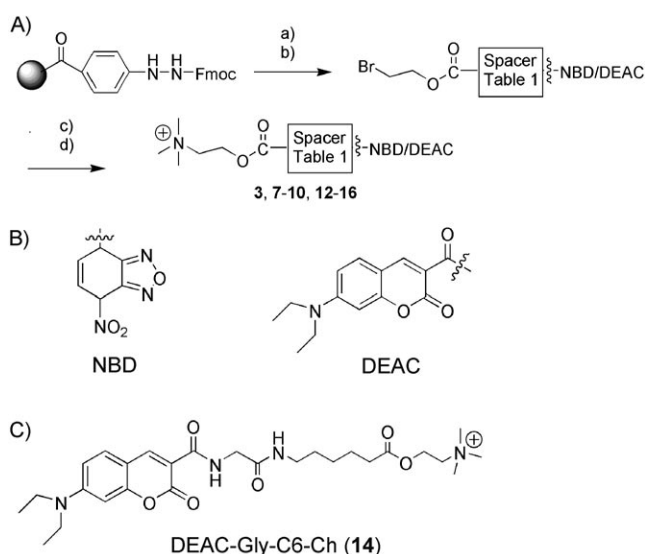
Scheme 1. A) Solid-phase synthesis of acylcholine-derived fluorophores: a) standard Fmoc peptide chemistry; b) bromoethanol, pyridine, Cu(OAc)$_2$, O$_2$, dichloromethane, 3 h, RT; c) sodium iodide in acetone, 6 h, reflux; d) trimethylamine in toluene, 72 h, RT. Structures of B) the environment-sensitive fluorophores used in this study and C) DEAC-Gly-C6-Ch (**14**).

Results and Discussion

Synthesis of fluorescent acylcholine derivatives with different linkers

We used a combination of solid-phase and solution-phase chemistry, based on described reactions,[17,18,30] for the syntheses of fluorescent acylcholines (Scheme 1 A, and Supporting Information). This synthesis strategy allowed us to provide a variety of fluorescent acylcholines possessing different linkers in adequate yields (μmol) and within a short time. The syntheses of fluorescent alkylcarbamate derivatives were performed by solution-phase chemistry (see Supporting Information). DEAC and NBD, both environment-sensitive dyes absorbing light above 400 nm, were chosen as fluorophores (Scheme 1 B). These fluorophores are suitable for a variety of fluorescence-based experiments such as fluorescence intensity, fluorescence resonance energy transfer, time-resolved fluorescence intensity, or flow cytometry.

Fluorescent acylcholine derivatives with improved pharmacological properties for the *Torpedo* nAChR

Initially, we tested the pharmacological properties of NBD-C6-Ch (**3**),[18] Dns-C6-Ch (**4**),[17,29] and DEAC-C6-Ch (**5**) because, like AC5 (**2**; for structure see the Supporting Information), they each possess an ε-aminohexanoic acid linker (Table 1). How-

Table 1. Summary of pharmacological data for functionalized acylcholines on recombinant *Torpedo* nAChR expressed in *Xenopus* oocyte.

Ligand[a]	Linker length[b]	I_{max}, EC$_{50}$, n_H[c]
ACh **1**	–	$100 \pm 5\%$ at 300 μm
		EC$_{50} = 25 \pm 4$ μm, $n_H = 1.6 \pm 0.2$
AC5 **2**[d]	8	100%
		EC$_{50} = 1.2$ μm, $n_H = 1.5$
NBD-C6-Ch **3**	6	$2.3 \pm 0.3\%$ at 100 μm
Dns-C6-Ch **4**	7	0.1% at 100 μm
DEAC-C6-Ch **5**	7	$1.0 \pm 0.3\%$ at 100 μm
DEAC-C4-CCh **6**	7	no current
NBD-C7-Ch **7**	7	$1.5 \pm 0.3\%$ at 300 μm
DEAC-Gly-Gaba-Ch **8**	8	$1.5 \pm 0.3\%$ at 50 μm
DEAC-Dae-Succ-Ch **9**	8	no current
NBD-βAla-Gaba-Ch **10**	8	$18 \pm 2\%$ at 100 μm
DEAC-C6-CCh **11**	9	no current
DEAC-Gaba-βAla-Ch **12**	9	$7 \pm 1\%$ at 50 μm
NBD-Gly-C6-Ch **13**	9	$30 \pm 4\%$ at 100 μm
DEAC-Gly-C6-Ch **14**	10	$50 \pm 3\%$ at 30 μm
		EC$_{50} = 3.4 \pm 0.4$ μm, $n_H = 2.1 \pm 0.2$
NBD-βAla-C6-Ch **15**	10	$11 \pm 1\%$ at 300 μm
NBD-Gaba-C6-Ch **16**	11	$50 \pm 5\%$ at 30 μm
		EC$_{50} = 5.4 \pm 0.6$ μm, $n_H = 2.0 \pm 0.2$

[a] AC5: (2-trimethylammonium)-ethyl-6-*N*-[*N'*-(methyl)-*para*-diazoniumphenylurea]hexanoate trifluoroacetate. Dae: diaminoethylene. Gaba: γ-aminobutyric acid. Succ: Succinate. [b] Number of atoms between the carbonyl group of the choline ester and the aromatic part of the chromophores; structures of the linkers see the Supporting Information. [c] I_{max}: maximum response relative to 300 μm. EC$_{50}$: concentration of half maximum activation. n_H: Hill coefficient. [d] Data from Mourot et al. 2006.[27] Number of experiments = 3–5, S.D. = 13.8%.

ever, these three fluorescent probes showed only very weak agonist activity on heterologously expressed *Torpedo* nAChR in relation to ACh (**1**). Aiming to develop fluorescent ligands with improved agonist efficiencies we synthesized two series of fluorescent acylcholines in which the linkers between the ACh binding unit and the environment-sensitive fluorophores (DEAC or NBD) were varied in length and structure (Table 1).

To avoid hydrophobic collapse, we introduced peptide bonds into longer linkers to make the spacers more hydrophilic, despite being more rigid.[31] In both series, the lengths and the molecular structures of the linkers connecting the choline and chromophore groups are the main attributes for the pharmacological activity. Ligands with the longest linkers (**13**–**16**) showed apparent efficacies of up to 50% relative to the maximum response of ACh on heterologously expressed *Torpedo* nAChR (Figure 1 A, inset). The EC$_{50}$ values determined were

A)

B)
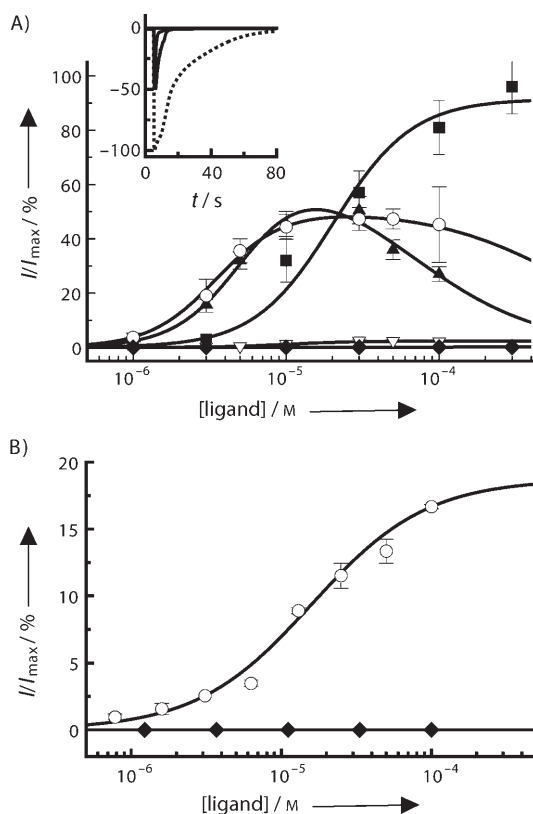
Figure 1. Dose–response relationships for different fluorescent acylcholines A) on wild-type *Torpedo californica* nAChR expressed in oocytes and B) on *Torpedo marmorata* nAChR transplanted on oocytes. Maximum responses are expressed in percentage relative to the maximum response with 300 μM ACh. ACh (■), DEAC-G-C6-Ch (○), NBD-Gaba-C6-Ch (▲), NBD-C6-Ch (▽), Dns-C6-Ch (◆). Solid lines represent fits to a modified Hill equation, which also accounts for noncompetitive inhibitor effects (see the Supporting Information). Inset: Normalized currents induced by ACh (300 μM; ⋯), DEAC-G-C6-Ch (30 μM; ——), and NBD-Gaba-C6-Ch (30 μM; -----). Error bars indicate the S.E.M. resulting from 3–5 measurements.

3.4 μM for **14** and 5.4 μM for **16**, which are comparable to the value previously found for the photolabel **2**[27] (Table 1). The pharmacological activities of the newly synthesized ligands are significantly higher than those of the commonly used fluorescent acylcholines **3** and **4** (Figure 1 A). Ligands with shorter linker lengths were not synthesized, since previous studies had found that they display no agonist activity.[17, 18, 29]

The observed weak pharmacological activities of **3** and **4** on heterologously expressed *Torpedo* nAChRs are particularly surprising because they contradict earlier results.[18, 29] However, direct comparison of new and previous results is difficult for several reasons. Firstly, the pharmacological characterization of the Dns- and NBD-containing ligands were originally performed on *Electrophorus electricus* electroplaques and on *Rana temporaria* sartorius muscle fibers, respectively, and nAChRs from different species might have distinct functional properties. Secondly, the experimental methodologies differed, because end-plate currents or potentials were measured and compared to the effect of 20 μM ACh, which is below the concentration needed for full activation of the receptor. Thirdly, the agonist effect was previously measured on native ion chan-

nels, and different pharmacological action may arise from differences in the expression system.[32–34] To ensure that we were working as close to native conditions as possible, we further characterized the pharmacological properties of **4** with the aid of voltage-clamp experiments on *Xenopus* oocytes transplanted with *Torpedo* membranes rich in nAChRs. This method keeps the receptors in their natural environment.[33] Again, for **14** we observed a maximal response and an EC_{50} value ($I_{max} = 19 \pm 2\%$, $EC_{50} = 15 \pm 3$ μM, $n_H = 1.1 \pm 0.1$), whereas no currents were detected with **4**, suggesting that this fluorescent acylcholine derivative behaves as an extremely weak agonist on *Torpedo* nAChR under the conditions used (Figure 1).

The different modifications made on the linker allowed us to gain some insight into the structure–activity relationship. Replacing the ester with a carbamate group (**6** and **11**) leads to a complete loss of pharmacological activity in *Torpedo* nAChR. All other fluorescent acylcholines show partial agonist behavior, with maximal efficacy for acylcholines with linkers containing ten to eleven atoms, with the exception of DEAC-Dae-Succ-Ch (**9**), which was pharmacologically inactive. These results suggest that the stereochemistry and flexibility of this position strongly influence the pharmacological activities of the fluorescent probes. In addition, the pharmacological action is completely lost if the spacer contains a succinyl building block **9**. DEAC-Gly-Gaba-Ch (**8**), NBD-βAla-Gaba-Ch (**10**), and DEAC-Gaba-βAla-Ch (**12**) show weak agonist behavior; this indicates that the positions and the orientations of the peptide bonds in the linkers strongly influence the physiological properties. Interestingly, the fluorescent acylcholines **14** and NBD-Gaba-C6-Ch (**16**) and the epibatidine-derived fluorescent agonists displaying full agonist behavior on a neuromuscular nAChR[28] have linkers of similar lengths.

The fluorescent agonists **14** and **16** show inhibitor effects at high concentrations with typical bell-shaped dose-response curves (Figure 1 A), similarly to other fluorescent acylcholines.[29] A detailed structure–activity relationship study has shown that fluorescent acylcholines mainly act as noncompetitive blocking agents, whereas aliphatic acylcholines of different lengths exhibit increased agonist character.[29] The aromatic chromophore might therefore interact with the receptor through hydrophobic, charge, or dipole interactions, resulting in inhibition of ion conduction at high ligand concentrations. In agreement with this observation, we detected current inhibition when ACh was co-applied with 100 μM NBD- or DEAC-dyes (data not shown).

DEAC-G-C6-Ch binds to desensitized *Torpedo* nAChR with nanomolar affinities, as shown by competitive radioligand binding

The nAChR is an allosteric receptor, and agonist binding induces conformational transitions with additional increases in affinity for the binding sites.[3] The binding affinity of the agonist ACh changes from the micromolar range for the basal state to the nanomolar range for the desensitized state. We characterized the binding properties of **14** for both states by using competition experiments against $[^{125}I]$-α-BgTx initial binding

rates. The binding affinity for desensitized nAChR was determined in the presence of the channel blocker proadifen (100 μM), conditions under which the receptor is mainly desensitized.[35] Protection constants of 22 ± 5 μM and 10 ± 2 nM were determined for the native and the desensitized states, respectively, revealing a shift of three orders of magnitude during desensitization. Such dramatic variations in affinities, which are expected for agonists, have been described for ACh[36] and can be explained by the allosteric behavior of the nAChR.[11]

DEAC-G-C6-Ch binding to *Torpedo* nAChR induced a strong increase in fluorescence intensity

The high affinity of **14** allowed the titration of the ligand with excesses of receptor binding sites. Baseline-corrected fluorescence emission spectra of free and completely titrated fluorescent ligand are shown in Figure 2. Complete saturation of fluo-
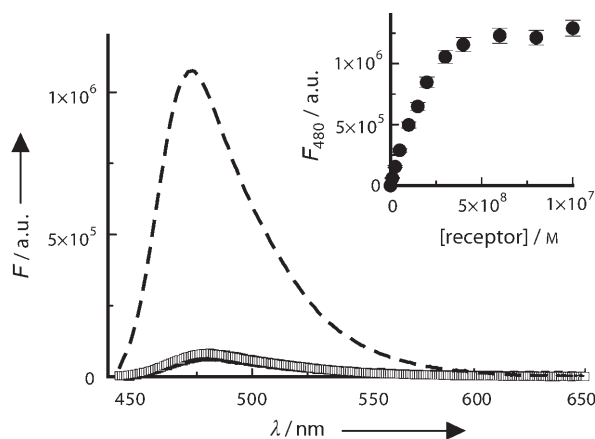
Figure 2. Baseline-corrected fluorescence emission spectra of DEAC-G-C6-Ch (10 nM, □), DEAC-G-C6-Ch (10 nM) in the presence of desensitized nAChR (90 nM, -----), and DEAC-G-C6-Ch (10 nM) in the presence of desensitized nAChR (90 nM) and of the non-fluorescent competitor CCh (100 μM, ■). The excitation wavelength was 430 nm. Inset: Titration curve of DEAC-G-C6-Ch (10 nM) with increasing amounts of desensitized nAChR.

rescent ligand (10 nM) by nAChR leads to a twelvefold enhancement of fluorescence intensity and a slight blue shift of the fluorescence emission maximum from 478 nm to 473 nm. Addition of excess nonfluorescent competitor CCh decreased the fluorescent signal to that of the free ligand, showing that the enhancement of fluorescence intensity was specifically associated with binding.

DEAC is well known as an environment-sensitive fluorophore and has been used in ligand–receptor binding studies.[37,38] In those studies, binding of DEAC-containing ligands induced strong enhancements of the fluorescence intensities due to specific ligand–receptor interactions. As shown in detailed photophysical studies, an increase in fluorescence intensity and a blue shift of the fluorescence maximum can be attributed to changes in the dipole moment and in the electronic structure, due to an increase in the solvent hydrophobicity of the surrounding medium.[39] In aqueous medium, DEAC-con-

taining acylcholines exhibit fluorescence quantum yields of 0.026 (Table 2) with fluorescence emission maxima at 478 nm, comparable with other DEAC-containing ligands.[37] In protic

Table 2. Comparison of spectroscopic and binding properties of different fluorescent acylcholine derivatives for the desensitized *Torpedo* nAChR.

Ligand Conditions	DEAC-G-C6-Ch TS, pH 7.0	Dns-C6-Ch TS, pH 7.0	NBD-C6-Ch[a] TS, pH 6.8
Fl QY free ligand	0.026 ± 0.002	$0.035^{[b]}$	0.019
K_p (native) [μM]	22 ± 5	n.d.	n.d.
K_p (D state) [nM]	10 ± 2	n.d.	n.d.
k_{ass} (D state) [M^{-1} s^{-1}]	$2.4 \pm 0.1 \times 10^7$	$4.0 \pm 0.3 \times 10^7$	n.d.
k_{diss} (D state) [s^{-1}]	0.012 ± 0.002 0.36 ± 0.04	0.10 ± 0.01 0.60 ± 0.05	0.23 0.064
K_D (D state) [nM]	0.5 ± 0.1 15.0 ± 2.5	2.5 ± 0.5 15.0 ± 3.0	1.2 10

[a] All data were obtained from Prinz and Maelicke.[22b] [b] Martinez et al.[24] Number of experiments = 2–3, S.D. = 13.7%.

organic solvents (ethanol, butan-1-ol) the fluorescence quantum yields of DEAC-containing acylcholines are significantly increased and the fluorescence emission maxima are blue-shifted (data not shown), an observation consistent with results obtained with other 7-(dialkylamino)coumarin dyes.[39] These results suggest that DEAC-G-C6-Ch occupies a more hydrophobic environment in the receptor bound state.

Association kinetics of DEAC-G-C6-Ch with desensitized torpedo nAChR

Employing enhancement of fluorescence intensity as an indicator of specific binding to nAChR, we performed kinetic experiments to determine the association rate constant of **14** with desensitized receptor. Figure 3 A shows association kinetics of **14** with desensitized nAChR (2 nM) at different ligand concentrations (3.6–145 nM). Increasing the concentration leads both to an acceleration of the association reaction and to an increase in the signal amplitude. No enhancement of fluorescence intensity was observable in the presence of an excess of non-fluorescent competitor CCh, affirming the specificity of the fluorescence signal.

Association of **14** to desensitized nAChR is well described by a single-exponential process for all ligand concentrations above 10 nM (Figure 3 A), as would be expected for pseudo-first-order conditions. Kinetics for ligand concentrations below 10 nM were not analyzed, due to the unambiguous existence of second-order conditions. However, *Torpedo* nAChR carries two agonist binding sites,[10] which might lead to more complex association kinetics. The observed single-exponential association kinetics suggest that the association processes are similar for both binding sites. Indeed, we could not detect any second kinetic phase, which could reflect differences in the association mechanism at the two binding sites.
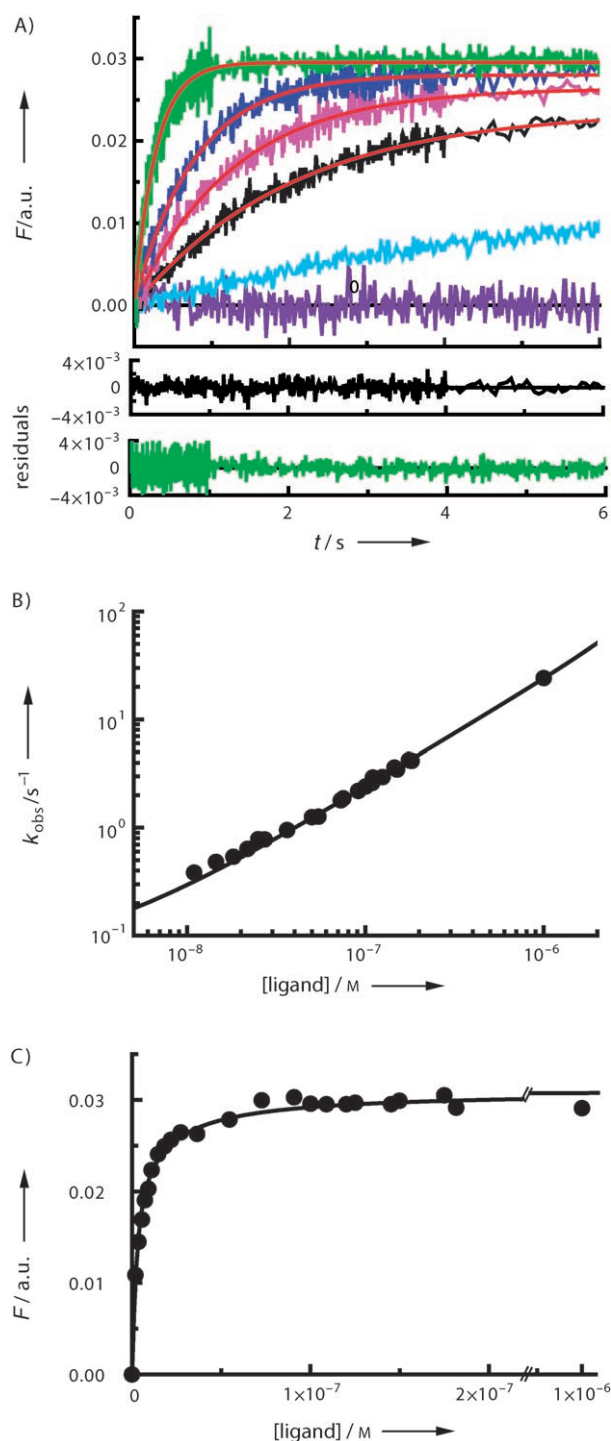
Figure 3. A) Time-course of DEAC-G-C6-Ch association with desensitized *Torpedo* nAChR (2 nM) as recorded by changes in fluorescence intensity in the presence of 3.6 nM (——), 15 nM (——), 27 nM (——), 54 nM (——), and 145 nM (——) of ligand. The excitation wavelength was 436 nm. Additionally, single-exponential fits of the data (——) and the corresponding residuals for concentration of 15 nM (——) and 145 nM (——) are displayed. No interactions between fluorescent ligand and receptor occur in the presence of excess nonfluorescent CCh (——). B) Double-logarithmic plot representing the observed rate constant for DEAC-G-C6-Ch association with desensitized nAChR as a function of ligand concentration (10^{-8} to 10^{-6} M). The solid line represents a fit to Equation (3) with $k_{ass} = 2.4 \times 10^7$ M^{-1}s^{-1} and $k_{diss} = 0.10$ s^{-1}. C) Kinetic amplitudes of association as function of ligand concentration. The solid line represents a fit according to Equation (5) with an apparent dissociation constant $K_D = 3.0$ nM.

The observed rate constants for DEAC-G-C6-Ch association increase linearly with ligand concentration (Figure 3 B), revealing an apparent two-state binding reaction between the receptor binding sites and the ligand [Eq. (1), below]. We determined a bimolecular association rate constant of $(2.4 \pm 0.1) \times 10^7$ M^{-1}s^{-1} for both binding sites of the desensitized receptor, which is a value near the limit of diffusion for second-order association reactions.[40] A slightly enhanced association rate constant towards the desensitized receptor state ($k_{ass} = (4.0 \pm 0.1) \times 10^7$ M^{-1}s^{-1}) could be determined for **4** (Table 2), which is in good agreement with a previously reported value.[23] The differences in the apparent bimolecular association rate constants might arise from an greater hydration volume of **14** or from different interactions in the binding pockets.[40]

As previously mentioned, kinetic association experiments with **14** revealed further that the receptor binding sites were not fully occupied for ligand concentrations below 75 nM (Figure 3 C). The amplitudes deduced from association kinetics reveal a hyperbolic concentration dependence reaching saturation at 75 nM, suggesting that the fluorescent ligand interacts independently with both binding sites. We determined an apparent dissociation constant of 3 nM for both binding sites with the aid of a binding isotherm, which accounts for second-order conditions [Eq. (5), below]. No amplitude increase was observed for concentrations up to 1 μM, suggesting that no further fluorescent ligand binds to the receptor at low micromolar concentrations.

Dissociation kinetics of DEAC-G-C6-Ch from desensitized torpedo nAChR

To obtain an improved insight into the properties of the two binding sites we performed displacement reactions using DEAC-G-C6-Ch (200 nM), a concentration sufficient completely to saturate proadifen-desensitized receptor (Figure 3 B) and excess nonfluorescent competitor CCh (1.25 mM, $K_D = 25$ nM[36]) to initiate displacement of the fluorescent ligand. Under these conditions the observed displacement rate constant is determined solely by the dissociation process of the fluorescent ligand.[40] The displacement kinetics indicated a complex process, which is well described by a double-exponential equation [Eq. (4), below] with observed rate constants of $k_1 = 0.012 \pm 0.002$ s^{-1} and $k_2 = 0.38 \pm 0.05$ s^{-1} and their respective absolute amplitudes of $A_1 = 0.028$ and $A_2 = 0.014$ (Figure 4 A). The biphasic kinetics of the displacement reaction might have several causes, such as conformational heterogeneity of the receptor, coupled conformational dynamics, or heterogeneity in different binding sites. The complex kinetics cannot account for the dissociation of **14** from the ion channel binding site, because proadifen fully occupies it. Rather, the biphasic kinetics of dissociation arise from the two non-equivalent agonist binding sites.

In order to assign the kinetic phases to each ACh binding site, we performed displacement reactions in the presence and in the absence of the site-selective inhibitor d-tubocurarine (dTC). The dTC (1 μM) completely occupies the αγ-binding site ($K_D = 35$ nM), while the αδ-binding site is expected to be virtu-
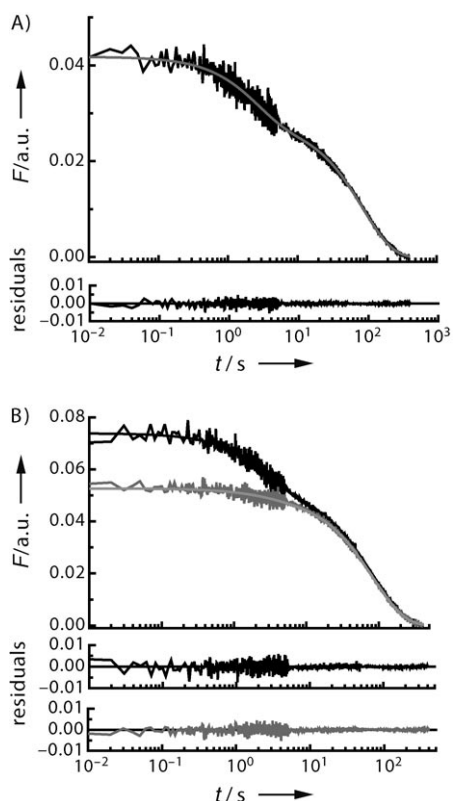
Figure 4. A) Displacement reaction (——) of DEAC-G-C6-Ch (200 nM) from proadifen-desensitized *Torpedo* nAChR induced by CCh (1.25 mM). The double-exponential fit of the data according to Equation (5) (——) and the corresponding residuals are displayed. The fit gives the following values: $A_1 = 0.028$, $k_1 = 0.012$ s^{-1}, $A_2 = 0.014$, and $k_2 = 0.38$ s^{-1}. B) Displacement reaction of DEAC-G-C6-Ch (100 nM) from *Torpedo* nAChR in the absence (——) and in the presence (——) of dTC (1 μM) induced by CCh (1.25 mM). Corresponding double-exponential fits and residuals are displayed. A global fit of the two kinetic traces gives the following values: in the absence of dTC: $A_1 = 0.051$, $k_1 = 0.012$ s^{-1}, $A_2 = 0.022$, and $k_2 = 0.34$ s^{-1}, and in the presence of dTC (1 μM): $A_1 = 0.050$, $k_1 = 0.012$ s^{-1}, $A_2 = 0.003$, and $k_2 = 0.34$ s^{-1}. The parameter k_2 was fixed due to the low amplitude A_2 in the case of dTC (1 μM).

ally free ($K_D = 1$–8 μM).[25,41,42] We were indeed able to block the αγ-binding site selectively with dTC (1 μM), as demonstrated by the disappearance of the fast kinetic phase of the displacement reaction (Figure 4B). The fast kinetic phase therefore most probably corresponds to the dissociation of **14** from the αγ-binding site, whereas the slow kinetic component relates to dissociation from the αδ-binding site.

The equilibrium dissociation constant (K_D) for each binding site can be determined from association and dissociation rate constants [Eq. (2), below]. The K_D values determined for **14** are 0.5 ± 0.1 nM for the αδ-binding site and 15.0 ± 2.5 nM for the αγ-binding site of the desensitized receptor, reflecting a strong site-selectivity. The subnanomolar affinity of **14** towards the αδ-binding site of desensitized *Torpedo* nAChR is the lowest value observed for functionalized acylcholines, indicating an extremely slow dissociation of the ligand from the αδ-binding site ($\tau > 80$ sec). For **3** and **4**, significantly faster dissociation rate constants were described, indicating weaker binding affinities towards the desensitized receptor (Table 2).

Thanks to their improved pharmacological and spectroscopic properties the newly described fluorescent acylcholines are perfect tools for the characterization of the microscopic rate and equilibrium constants for binding and gating on *Torpedo* nAChR, ideally by use of a combination of fluorescence and electrophysiology techniques. The complete identification and description of the microscopic reaction steps will provide essential information for the successful description of the actions of agonists, antagonists, and allosteric modulators, as well as for improved identification of new pharmacologically active compounds.

Conclusions

We have examined the pharmacological properties of a series of fluorescent acylcholine derivatives with respect to *Torpedo* nAChR and have identified highly efficacious fluorescent agonists. Additionally, we have determined binding and spectroscopic properties of the most prominent fluorescent acylcholine—DEAC-G-C6-Ch—on desensitized nAChR. The main findings are: 1) the newly synthesized fluorescent acylcholines are much more efficacious than the commonly used fluorescent derivatives NBD-C6-Ch (**3**) and Dns-C6-Ch (**4**), and 2) DEAC-G-C6-Ch (**14**) displays a strong site selectivity with desensitized *Torpedo* nAChR, binding with subnanomolar affinity to the αδ-binding site and with nanomolar affinity to the αγ-binding site.

Experimental Section

Materials: Unless otherwise noted, reagents and chemicals were obtained from Aldrich, Bachem, Fluka, Novabiochem, or Sigma. Small live *Torpedo marmorata* fish were obtained from the Biological Station of Roscoff (France). Adult female *Xenopus laevis* frogs were obtained from the Centre d'élevage de Xénopes (Université de Rennes) and were maintained and treated according to European standard protocols approved by our institutional animal care and use committees. [^{125}I]α-Bungarotoxin ([^{125}I]α-BgTx) was purchased from New England Nuclear.

Synthesis of fluorescent acylcholine derivatives: See the Supporting Information.

(3-(7-Diethylaminocoumarin)carbonyl)glycyl 6-amino-hexanoic acid β-(N-trimethylamino)ethyl ester, DEAC-G-C6-Ch (14): ^{1}H NMR (D$_2$O): $\delta = 1.16$ (t, 6H), 1.40 (d, 2H), 1.58–1.69 (m, 4H), 2.41 (t, 2H), 3.17 (m, 11H), 3.38–3.42 (d, 4H), 3.68 (s, 2H), 4.01 (s, 2H), 4.49 (s, 2H), 6.35 (s, 1H), 6.64–6.70 (d, 1H), 7.29–7.33 (d, 1H), 8.28 ppm (s, 1H); MS: see the Supporting Information.

Steady-state fluorescence measurements: Measurements were taken in PBS containing Triton X-100 (0.01%) and proadifen (100 μM). Fluorescence measurements were obtained on a Fluorolog fluorimeter with a xenon lamp source. Fluorescent probes were excited at 430 nm, selected by an excitation monochromator with a 4 nm slit width. The emission spectra were recorded between 440 and 650 nm by use of an emission monochromator with a 4 nm slit width. Fluorescence quantum yields were determined as described.[28]

Stopped-flow fluorescence measurements: All kinetic measurements were performed at 20 °C in "*Torpedo*" buffered saline (TS)

[phosphate (5 mм, pH 7.0), NaCl (250 mм), KCl (5 mм), CaCl$_2$ (4 mм), MgCl$_2$ (2 mм)] in the presence of phenylmethylsulfonyl fluoride (PMSF, 1 mм) and proadifen (100 μm). Experiments were carried out on a SFM-300 stopped-flow fluorescence instrument from Bio-Logic (Claix, France) fitted with a xenon lamp light source and a temperature control unit. DEAC-containing probes were excited at 436 nm. The emission signal was collected through a 455 nm cut-off filter (Melles Griot). Fluorescence energy transfer from nAChR to Dns-C6-Ch was monitored by use of an excitation wavelength of 280 nm, and Dns emission was collected through a 435 nm cut-off filter (Melles Griot).[20] Single mixing experiments to measure binding and dissociation kinetics were performed by mixing 1+1 volumes. Individual shots (4–8) were averaged to reduce noise.

Data analysis of association and displacement reactions: ProFit software (QuantumSoft, Zürich, Switzerland) was used for data evaluation. In the simplest case, free (L) and receptor-bound (RL) ligand interchange with the microscopic rate constants k_{ass} and k_{diss}:

$$R + L \underset{k_{diss}}{\overset{k_{ass}}{\rightleftharpoons}} RL \tag{1}$$

and the equilibrium dissociation constant (K_D) is expressed as:

$$K_D = \frac{[R][L]}{[RL]} = \frac{k_{diss}}{k_{ass}} \tag{2}$$

Association and displacement kinetics were used to determine the dissociation constants of DEAC-Gly-C6-Ch with the binding sites of desensitized nAChR. Kinetic traces of association reactions were analyzed by use of a single-exponential equation [Eq. (3)]. Under pseudo-first order conditions ([L]≫[RL]) and after perturbation from equilibrium the relaxation process for a two-state association reaction follows a single-exponential time course with the observed rate constant:

$$k_{obs} = k_{ass} \times [L] + k_{diss} \tag{3}$$

yielding association and dissociation rate constants.

Displacement reactions were performed under similar conditions in the absence and in the presence of dTC (1 μm). The concentration of dTC stock solution was determined by use of a molar extinction coefficient of $\varepsilon_{282} = 7500\ \text{м}^{-1}\text{cm}^{-1}$.[25] Proadifen-desensitized nAChR was preincubated with dTC (1 μm) for 1 h. Equilibration of DEAC-G-C6-Ch binding with desensitized nAChR in the absence and in the presence of dTC was performed for 30 min. Displacement of bound fluorescent ligand was initiated by the addition of an excess of the nonfluorescent competitor carbamoylcholine (CCh, 1.25 mм, $K_D = 25$ nм[36]). At this concentration of competitor the observed rate constant for displacement is fully determined by the dissociation process of the fluorescent ligand.[40] Kinetic traces were analyzed by use of a double-exponential equation:

$$F(t) = A_1 \times e^{-k_1 \times t} + A_2 \times e^{-k_2 \times t} + C \tag{4}$$

where F is the observed fluorescence intensity, k_1 and k_2 are the observed dissociation rate constants, and A_1 and A_2 are their corresponding fluorescence amplitudes. C represents the observed fluorescence signal at infinite time. Dissociation constants were independently calculated for the two binding sites according to Equation (3) with the assumption of similar association rate constants for the two binding sites.

Amplitudes obtained from association experiments were analyzed by using the following equation, which accounts for second-order conditions:

$$F([L]) = \frac{F_{max} \times A}{2 \times [R]} \times \left(K_D + [L] + [R] - \sqrt{(K_D + [L] + [R])^2 - 4[L][R]}\right) \tag{5}$$

where F_{max} is the maximal fluorescence intensity, A is the amplitude obtained from association kinetics experiments, and K_D is the corresponding dissociation constant obtained from kinetic experiments. [L] is the initial concentration of ligand, and [R] is the initial concentration of receptor.

For additional experimental procedures see the Supporting Information.

Acknowledgements

[1] M. B. Jackson, *Proc. Natl. Acad. Sci. USA* **1989**, *86*, 2199.
[2] A. Karlin, M. H. Akabas, *Neuron* **1995**, *15*, 1231.
[3] J. P. Changeux, S. J. Edelstein, *Neuron* **1998**, *21*, 959.
[4] S. M. Sine, A. G. Engel, *Nature* **2006**, *440*, 448.
[5] A. Mourot, T. Grutter, M. Goeldner, F. Kotzyba-Hibert, *ChemBioChem* **2006**, *7*, 570.
[6] D. Colquhoun, B. Sakmann, *Nature* **1981**, *294*, 464.
[7] S. M. Sine, T. Claudio, F. J. Sigworth, *J. Gen. Physiol.* **1990**, *96*, 395.
[8] C. Franke, H. Parnas, G. Hovav, J. Dudel, *Biophys. J.* **1993**, *64*, 339.
[9] A. Miyazawa, Y. Fujiyoshi, N. Unwin, *Nature* **2003**, *423*, 949.
[10] N. Unwin, *J. Mol. Biol.* **2005**, *346*, 967.
[11] S. J. Edelstein, O. Schaad, E. Henry, D. Bertrand, J. P. Changeux, *Biol. Cybern.* **1996**, *75*, 361.
[12] D. S. Dahan, M. I. Dibas, E. J. Petersson, V. C. Auyeung, B. Chanda, F. Bezanilla, D. A. Dougherty, H. A. Lester, *Proc. Natl. Acad. Sci. USA* **2004**, *101*, 10195.
[13] R. Hovius, P. Vallotton, T. Wohland, H. Vogel, *Trends Pharmacol. Sci.* **2000**, *21*, 266.
[14] C. Biskup, J. Kusch, E. Schulz, V. Nache, F. Schwede, F. Lehmann, V. Hagen, K. Benndorf, *Nature* **2007**, *446*, 440.
[15] J. B. Cohen, J. P. Changeux, *Biochemistry* **1973**, *12*, 4855.
[16] F. J. Barrantes, B. Sakmann, R. Bonner, H. Eibl, T. M. Jovin, *Proc. Natl. Acad. Sci. USA* **1975**, *72*, 3097.
[17] G. Waksman, M. C. Fournie-Zaluski, B. Roques, T. Heidmann, H. H. Grünhagen, J. P. Changeux, *FEBS Lett.* **1976**, *67*, 335.
[18] H. W. Meyers, R. Jurss, H. R. Brenner, G. Fels, H. Prinz, H. Watzke, A. Maelicke, *Eur. J. Biochem.* **1983**, *137*, 399.
[19] R. Jurss, H. Prinz, A. Maelicke, *Proc. Natl. Acad. Sci. USA* **1979**, *76*, 1064.
[20] T. Heidmann, J. P. Changeux, *Eur. J. Biochem.* **1979**, *94*, 255.
[21] T. Heidmann, J. Bernhardt, E. Neumann, J. P. Changeux, *Biochemistry* **1983**, *22*, 5452.
[22] H. Prinz, A. Maelicke, *Biochemistry* **1992**, *31*, 6728.
[23] D. E. Raines, N. S. Krishnan, *Biochemistry* **1998**, *37*, 956.

[24] K. L. Martinez, P. J. Corringer, S. J. Edelstein, J. P. Changeux, F. Merola, *Biochemistry* **2000**, *39*, 6979.

[25] X. Z. Song, I. E. Andreeva, S. E. Pedersen, *Biochemistry* **2003**, *42*, 4197.

[26] I. E. Andreeva, S. Nirthanan, J. B. Cohen, S. E. Pedersen, *Biochemistry* **2006**, *45*, 195.

[27] A. Mourot, J. Rodrigo, F. Kotzyba-Hibert, S. Bertrand, D. Bertrand, M. Goeldner, *Mol. Pharmacol.* **2006**, *69*, 452.

[28] J. Grandl, E. Sakr, F. Kotzyba-Hibert, F. Krieger, S. Bertrand, D. Bertrand, H. Vogel, M. Goeldner, R. Hovius, *Angew. Chem.* **2007**, *119*, 3575; *Angew. Chem. Int. Ed.* **2007**, *46*, 3505.

[29] G. Waksman, J. P. Changeux, B. P. Roques, *Mol. Pharmacol.* **1980**, *18*, 20.

[30] B. Chatrenet, F. Kotzba-Hibert, C. Mulle, J. P. Changeux, M. P. Goeldner, C. Hirth, *Mol. Pharmacol.* **1992**, *41*, 1100.

[31] P. J. Flory, *Statistical Mechanics of Chain Molecules*, Hanser, Munich, Germany, **1968**.

[32] F. J. Barrantes, *Faseb J.* **1993**, *7*, 1460.

[33] A. Morales, J. Aleu, I. Ivorra, J. A. Ferragut, J. M. Gonzalez-Ros, R. Miledi, *Proc. Natl. Acad. Sci. USA* **1995**, *92*, 8468.

[34] T. M. Lewis, P. C. Harkness, L. G. Sivilotti, D. Colquhoun, N. S. Millar, *J. Physiol.* **1997**, *505*, 299.

[35] E. K. Krodel, R. A. Beckman, J. B. Cohen, *Mol. Pharmacol.* **1979**, *15*, 294.

[36] N. D. Boyd, J. B. Cohen, *Biochemistry* **1980**, *19*, 5344.

[37] M. R. Webb, G. P. Reid, V. R. Munasinghe, J. E. Corrie, *Biochemistry* **2004**, *43*, 14463.

[38] P. Zhuang, A. I. Chen, C. B. Peterson, *J. Biol. Chem.* **1997**, *272*, 6858.

[39] B. B. Raju, T. S. Varadarajan, *J. Phys. Chem.* **1994**, *98*, 8903.

[40] H. Gutfreund, *Kinetics for the Life Sciences: Receptors, Transmitters and Catalysts*, Cambridge University Press, **1995**.

[41] R. R. Neubig, J. B. Cohen, *Biochemistry* **1979**, *18*, 5464.

[42] S. E. Pedersen, J. B. Cohen, *Proc. Natl. Acad. Sci. USA* **1990**, *87*, 2785.